E1-94-436

J.Budagov, I.Chirikov-Zorin, V.Glagolev,
A.Pantea[1], D.Pantea[1], S.Tokar[2]

# EFFECT OF NONUNIFORMITY
# ON THE ENERGY RESOLUTION
# OF E.M. SAMPLING CALORIMETERS

[1]Permanent address: Institute of Atomic Physics, P.O.Box MG-6,
Bucharest, Romania
[2]Comenius University of Bratislava, Slovakia

1994

# 1   Introduction

The calorimeters have been used extensively in high energy physics experiments in the last decade and they will play a significant role at the new detectors designed to operate at energies in the TeV range at future supercolliders. At these energies the electromagnetic sector of the calorimeter might play an important role in the search of the new physics, for example in the identification of Higgs boson production signals from $H \to \gamma\gamma$ decays.

The observation of such signals requires very good energy resolution and, in order to obtain it, all factors which might influence the value of resolution must be taken into account. Going to higher energies, the behaviour of the energy resolution changes; it is no more dominated by sampling effects, but by the systematic effects such as response nonuniformity of sensitive elements, finite containment, intercell calibration, energy leakage [1]. So that, a more detailed study of the influence of these effects becomes now necessary.

Usually, if the electronics noise is not taken into account, the energy resolution is parametrized by a quadratic addition of a Poisson-like term due to effects such as sampling and photostatistics and of a constant term due to systematic effects:

$$\frac{\sigma}{E} = \frac{a}{\sqrt{E}} \oplus b \quad . \tag{1}$$

According to our present understanding, all the above-mentioned systematic effects, expected to dominate the behaviour of energy resolution at very high energies, will contribute to $b$-term from equ (1). However the concrete form of the $b$-term dependence on each of these effects remains still to be studied.

In the present paper we have investigated how the tile to tile nonuniformity influences the energy resolution of a sampling tile electromagnetic calorimeter, in our case a sampling calorimeter using scintillator plate with wavelength-shifting fiber readout as a sampling medium and lead as an absorber. This type of calorimeter was considered as one of the possible options for calorimetry (electromagnetic or hadronic) at future supercolliders. To be able to isolate the nonuniformity effects, some parameters of the calorimeter which was simulated in this paper were deliberately exaggerated in order to switch-off the contribution of other systematic effects. For example, to remove the effect of the energy leakage, the dimensions of the calorimetric tower were chosen much larger than they are in real calorimeters.

In the first section the notations used in the paper are introduced and explained. Some details are given on the Monte-Carlo simulation of what will be called the ideal case and on the way the tile to tile response nonuniformity is taken into account. A qualitative description of the tiles nonuniformity influence on the energy resolution is given. It results that in $b$, the systematic term, there are two components: an intrinsic one and a component which depends on the calibration.

In the next section some previously obtained analytical results concerning the $b$ term calibration component are reviewed. Different calibration procedures are then applied to the simulated data, that are calibrated either globally, or tower by tower in order to test the qualitative description given in the first section. It is shown that the contribution of the tile to tile nonuniformity to the $b$-term increases linearly with $\sigma_{non}$, the standard deviation of nonuniformity. The observed deterioration of the energy resolution, due to nonuniformity, can be restricted inside resonable limits if the tower by tower calibration is used. A good agreement between the simulation and analytical computations is found.

Finally, in the third section the conclusions are presented.

# 2 Monte Carlo simulation

## 2.1 Ideal case

Firstly, it was simulated what will be called in the following the ideal case, i.e. a sandwich-tile calorimeter tower, whose dimensions are chosen large enough to avoid any energy leakage (longitudinal, transversal) and where the tiles are identical regarding their response.

The calorimeter tower considered in the simulation program consisted of a stack of alternative layers of absorber (lead) and plastic scintillator. The lead and scintillator plates were chosen to have identical 0.4 $cm$ thickness and $30 \times 30$ $cm^2$ transversal dimensions. The tower is composed from $N_{tile} = 64$ of such pairs of absorber/scintillator plates, which corresponds to a total tower length of 51.2 $cm$, or 46.2 radiation lengths.

The GEANT program [2] version 3.15 was used to simulate the electromagnetic showers produced in this tower by an electron beam at nine values of the incident energy: 10, 20, 50, 100, 150, 200, 300, 400 and 500 $GeV$. The incident beam direction is perpendicular to the tiles surface and the incidence point is just in the tile center. The energy cuts for both electrons and gammas were traced down to 10 $KeV$, the limit permitted by the actual version of the GEANT program. The simulations were performed on a SUN workstation and the mean computing time was 1.8 sec/event/GeV.

In what follows, by $E_i$ it is denoted the deposited energy in the $i^{th}$ tile. As a result of our GEANT simulation, for one incident electron, the output consisted of the set $\{E_i, i = 1, N_{tile}\}$ of deposited energies in all scintillator layers of the tower. Their sum:

$$S = \sum_{i=1}^{Ntile} E_i \tag{2}$$

will be called a calorimetric signal, and it characterises the calorimeter response to an individual electron, which in the ideal case is strictly related to the amount of deposited energy in the tiles. The distribution of the signals simulated at a definite value of the incident energy is Gaussian. The tower energy resolution is given as the ratio of the standard deviation to the mean value of this distribution.

A summary of the number of simulated electromagnetic showers and of the energy resolution obtained at each of the nine above-mentioned energies can be found in Table I.

**Table I** The energy resolution in the ideal case

| Energy [GeV] | No. of simulated events | Resolution [%] |
|:---:|:---:|:---:|
| 10 | 1000 | $3.95 \pm 0.09$ |
| 20 | 1000 | $2.77 \pm 0.06$ |
| 50 | 1000 | $1.72 \pm 0.04$ |
| 100 | 600 | $1.24 \pm 0.04$ |
| 150 | 500 | $0.99 \pm 0.03$ |
| 200 | 325 | $0.80 \pm 0.03$ |
| 300 | 300 | $0.73 \pm 0.03$ |
| 400 | 300 | $0.60 \pm 0.02$ |
| 500 | 300 | $0.56 \pm 0.02$ |

For the ideal calorimeter, taking into account that in this case there is only the sampling phenomenon which contributes to the energy resolution, one should expect for it to behave like $a/\sqrt{E}$. Therefore, by fitting the Table I values with the general formula given by equ. (1), we ought to obtain for $b$ a value consistent with zero, and this is obtained indeed. In fig. 1 the energy dependence of the energy resolution, with $1/\sqrt{E}$ on the abscissa, is represented. With squares are represented data points and with continuous line is drawn the energy dependence as predicted by equ.(1), with fitted values of the parameters $a$ and $b$: $a = 12.23 \pm 0.12\%$ and $b = 0.00 \pm 0.12\%$ for $\chi^2/ndf = 0.92$.

## 2.2    Inclusion of the tile to tile nonuniform response

The tile response nonuniformity is introduced "by hand" over the simulated in the ideal case deposited energies for each event. In GEANT simulation all scintillator layers were considered identical, which is not very far from the quality provided by the manufacturers. The imperfections from the machining of the groves in the scintillator plates or damages of the wavelength shifting fibers during the operation of their insertion inside these groves may affect the reproducibility of the light output among the tiles.
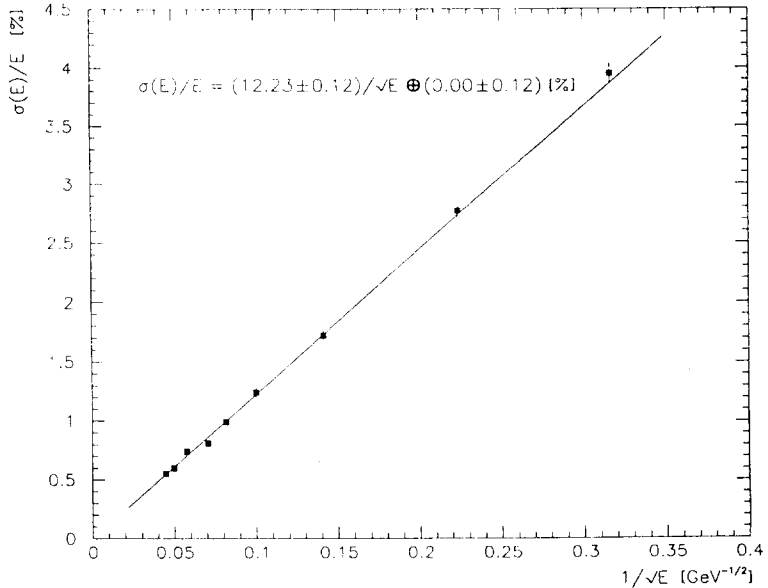
**Fig. 1** . Energy resolution $\sigma(E)/E$ vs. $1/\sqrt{E}$ from Monte Carlo simulation of the ideal case.
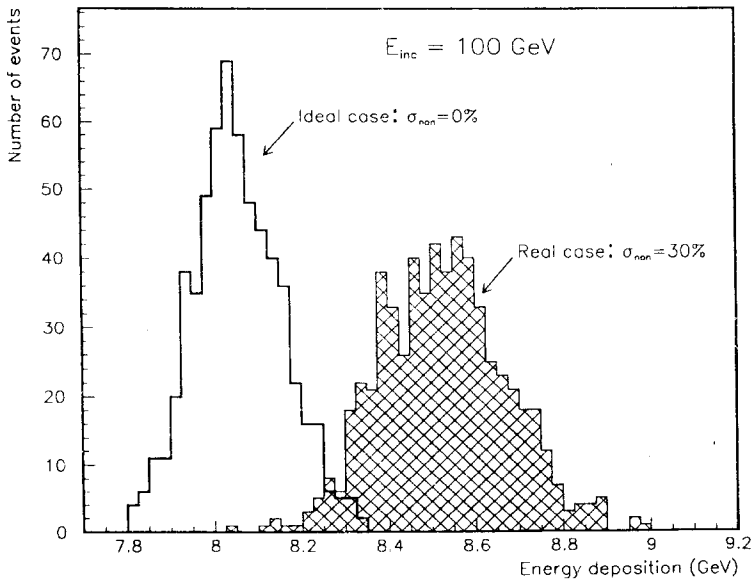


**Fig. 2** . An illustration of the tile to tile nonuniformity effects for the distribution of calorimetric signal in a random tower in the ideal case and in $\sigma_{non} = 30\%$ real case.

The GEANT simulation results in the ideal case were stored in separate files for each energy. The $i^{th}$ tile response nonuniformity is introduced in a form of a coefficient $C_i$ which weights the energy deposition in that tile. The calorimeter signal in this case, which in the following will be called "the real signal", now reads:

$$S = \sum_{i=1}^{Ntile} C_i E_i \quad . \tag{3}$$

The coefficient $C_i$ characterises the conversion efficiency of the deposited energy in the $i^{th}$ tile into a light signal. The set $\{C_i, i = 1, N_{tile}\}$ characterises an individual calorimeter tower and equ.(3) is used to compute its real signal to each simulated event at all energies.

In this paper, the tile nonuniformity is considered to be Gaussian distributed with standard deviation $\sigma_{non}$. The standard deviation is interpreted as a measure of the nonuniformity. Such an approach is justified in the case when the tiles individual characteristics are not measured separately and the calorimeter towers are assembled without any selection of the tiles. With this considerations, the $C_i$ coefficients can be defined as:

$$C_i = 1 + \sigma_{non} r_i \quad . \tag{4}$$

where:

- $r_i$ is a random number generated according to the standard Gaussian distribution;

- $\sigma_{non}$ is the tile response standard deviation, characterising the degree of nouniformity, or the quality of the tile party.

About the use of a global coefficient $C_i$ to characterise the tile response, some comments are in order. The response variations of a tile at different points on its surface are observed from measurements made using collimated radioactive sources [3] and the effect is important in the case of electromagnetic showers. In practice there are already invented some ways to reduce this unpleasant phenomenon, for example by the use of a suitable response flattening mask. In this way, the response variation across the tile surface may be reduced at the level of about 3% or less [3]. Therefore, our simplification, of using a single coefficient $C_i$ and not a function of the coordinates $(x, y)$ on the tile surface to describe the characteristics of its light output, goes not very far from the real situation.

In order to investigate the effect of the nonuniformity, we assume to have several calorimeter towers, each of them characterised by its own set of the tower response coefficients $\{C_i, i = 1, N_{tile}\}$. We can reconstruct, using equ.(3), the response of any tower at any incident energy (the real signal) using the bank of the simulated ideal case events at this energy and the set of its response coefficients $C_i$. From the

5

real signal distribution for all generated events at a given energy one can obtain the tower resolution at this energy. In the ideal case all the towers are identical and the tower energy resolution coincides with the value of the calorimeter resolution. In the real case the nonuniformities are statistically distributed and different values of energy resolution are obtained for different towers.

Therefore, in the real case the calorimeter resolution cannot be identified with the resolution of a tower. It has to be defined as a global characteristic of whole calorimeter. Our choice was to define the calorimeter energy resolution from its averaged response obtained over all towers that compose it. In other words we considered the calorimeter response for different incident points distributed on the whole calorimeter surface in the center of its towers. In order to calculate the energy resolution we need to compute the real response of a large number of different towers and then to treat them in the frame of a certain calibration procedure (see bellow). In this paper we have computed the responses of 1000 different towers using, for each tower, a different set of response coefficients $\{C_i, i = 1, N_{tile}\}$, generated according to formula (4), and the banks of simulated ideal case events for all incident energies.

In order to study the dependence of the energy resolution on the tile response nonuniformity $\sigma_{non}$, for each tower were generated five independent sets of response coefficients, each set being characterised by a different value of $\sigma_{non}$: 5, 10, 15, 20 and 30%.

The nonuniformity affects the real signal distribution in two ways: by a shift of the mean value and by an increase of its width, while the distribution itself remains Gaussian. For illustrative purposes, the distribution of the ideal signal and that of a particular tower real signal for $\sigma_{non} = 30\%$ at the incident energy $E_{inc} = 100$ GeV are shown in fig. 2. The mean value $\overline{E}$ and the standard deviation $SD$ of these two distributions are: $\overline{E} = 8.056 \pm 0.004$ GeV and $SD = 0.102 \pm 0.004$ GeV for the ideal case and $\overline{E} = 8.523 \pm 0.003$ GeV and $SD = 0.141 \pm 0.005$ GeV for the real case. In the real case the magnitude of the effect differs from tower to tower and depends also on the nonuniformity $\sigma_{non}$. In fig. 3 the distributions of the $\overline{E}$ values (fig. 3a) and of $SD$ (fig. 3b) for all the 1000 towers are plotted at two values of $\sigma_{non}$: 10% and 30%.

Therefore, we expect these two effects to influence each in its own way the energy resolution $b$ term and to contribute to it with two independent terms. The shift of the mean value could be corrected by different calibration procedures, so we called its contribution *calibration term* and denoted it by $b_c$. The other contribution, due to the broadening of the calorimetric signal distribution, cannot be influenced by calibration, so we called it *intrinsic term* and denoted by $b_0$.

The effect of the calibration is considered in detail in the next section.
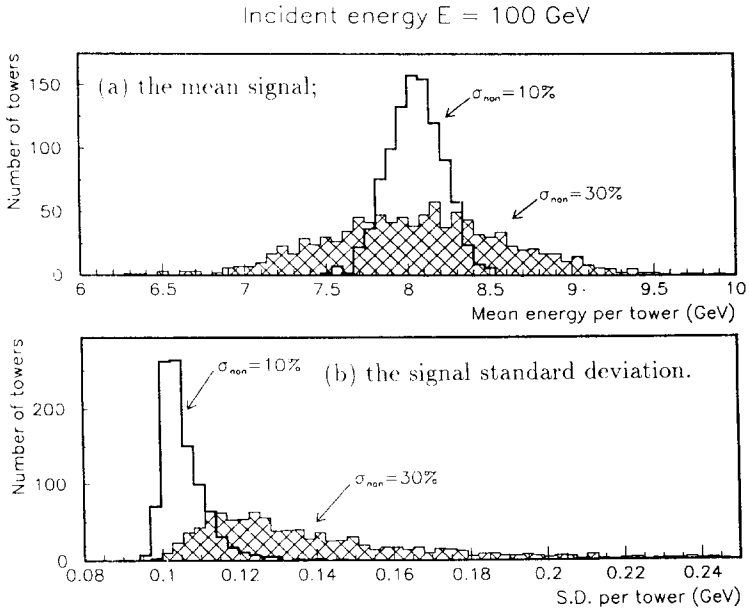
6

**Fig. 3.** Distribution over the whole calorimeter surface of the signal characteristics per tower for $\sigma_{non} = 10\%$ and $\sigma_{non} = 30\%$.
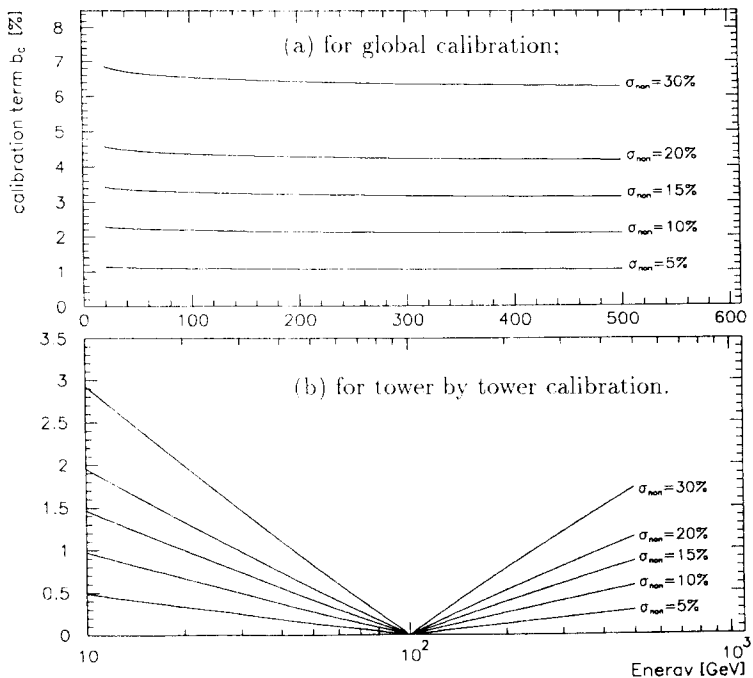


**Fig. 4.** Predicted $b_c$ energy dependence for various nonuniformity values $\sigma_{non}$.

# 3   Calibration

By calibration we mean a correspondence, established between the calorimeter signal and the incident electron energy. In our case this correspondence takes a very simple form:

$$E = KS \quad , \tag{5}$$

where $K$ is the calibration coefficient, $S$ the calorimeter signal and $E$ the reconstructed energy.

Assuming a calorimeter linear response, the calibration coefficient $K$ is given by the ratio of the calibration energy $E_0$ to the average signal $\overline{S}$

$$K = \frac{E_0}{\overline{S}} \quad . \tag{6}$$

We discuss two situations: a global calibration when a unique calibration coefficient $K$ is used to calibrate all towers, and a tower by tower calibration , when for each tower is used its own calibration coefficient. In addition we also use the term of absolute calibration, to designate a special procedure which will be defined later and that was introduced in order to help us in our analysis.

In our previous paper [4] some analytical expressions were obtained for the calibration term $b_c$ in global and in tower by tower calibration. The universal parametrisation of the electromagnetic shower mean longitudinal profile by a gamma distribution [5]:

$$\frac{dE}{dt} = E_{inc} \frac{\beta}{\Gamma(\alpha)} (\beta t)^{\alpha-1} e^{-\beta t} \tag{7}$$

was used there to compute the calorimeter signal. The parameters $\alpha$ and $\beta$ contain the shower profile energy dependence. For instance, for electron induced showers:

$$\beta \simeq 0.5: \quad \frac{\alpha - 1}{\beta} = \ln y + C_e \quad , \tag{8}$$

where $C_e = -0.5$ [5], or $C_e = -1.0$ [6], but choosing one or another of the $C_e$ values will little affect our results. As in [4] we used here $C_e = -1.0$.

The shower parametrisation is expressed in the scaled variables $y$ and $t$ [5]:

$$y = \frac{E_{inc}}{E_c}; \quad t = \frac{x}{X_0} \tag{9}$$

with $y$, the incident energy, measured in units of the calorimeter averaged material critical energy $E_c$ and $t$, the coordinate along the shower axis, considered relative to the front edge of the calorimeter, and expressed in radiation lengths $X_0$ of the calorimeter averaged material.

After global or tower by tower calibration of the calorimeter signal one obtains [4] that $b$ term is not a constant, but it has a slow dependence on energy. For global calibration the following dependence was predicted [4]:

$$b_c^{gl} = \sigma_{non}(\Delta t)^{1/2}\left(\frac{\beta}{4\pi \ln y}\right)^{1/4} \quad , \tag{10}$$

where $\Delta t$ is the thickness of an averaged medium layer composed from one layer of lead plus one layer of scintillator, measured in units of the average radiation length $X_0$.

Assuming that we calibrated tower by tower at the energy $E_0$, the following expression was found in [4] for the energy dependence of the $b_c^{tw}$:

$$b_c^{tw} = \sigma_{non}(2\pi \Delta t)^{1/2}\left(\frac{\beta}{4\pi \ln y_0}\right)^{3/4}\left|\ln\left(\frac{E}{E_0}\right)\right| \quad . \tag{11}$$

where $y_0$ represents the calibration energy expressed in the scaled variable $y$.

The $b_c$ term energy dependence, is illustrated in the fig. 4 for the case of calorimeter simulated in previous section, namely for global calibration in fig. 4a and for tower by tower calibration in fig. 4b. The numerical values of different parameters entering in the expressions for $b_c^{gl}$ and for $b_c^{tw}$ given above are: $E_c = 10.48\ MeV$, $\Delta t = 0.72$ and calibration energy $E_0 = 100\ GeV$.

In this section, our goal was that for the $b$ term, obtained from the simulated data sample, to separate the intrinsic $b_0$ and calibration $b_c$ components, to study their dependence on the nonuniformity $\sigma_{non}$ and to compare the found values with the values predicted in [4].

In the following, equ. (11) is written in the form:

$$b_c^{tw} = c\left|\ln\left(\frac{E}{E_0}\right)\right| \quad . \tag{12}$$

and in the comparison with simulated data the logarithmic dependence on energy and the $c$ coefficient linear dependence on $\sigma_{non}$ is checked.

As it can be seen from fig. 4b, $b_c^{tw}$ is zero at the calibration energy $E_0$. This result looks very plausible, because the tower average signal shift in respect with the mean signal in the ideal case could be completely compensated only at that energy where the tower is for these shifts at the level of the whole calorimeter may happen only when each of the towers is calibrated individually. At another energy, a total correction cannot be achieved because the mean shower profile depends on energy and in consequence the different tiles relative contribution to the calorimetric signal changes also with energy. The shower profile energy dependence is slow, of logarithmic type, therefore it was also expected for the $b_c^{tw}$ value to depend on energy in the same manner. As regards the intrinsic term we made the assumption that it doesn't depend on energy.

9

The equ.(11) prediction that $b_i^{nv} = 0$ at $E = E_0$ is used to separate in the $b$ term the calibration contribution from the intrinsic one. We proceeded calibrating tower by tower simultaneously at all the energies. At each energy where the tower was calibrated, only intrinsic effects will contribute to the $b$ term. In the following we will refer to this procedure as to an absolute calibration. In Table II the values of the calorimeter energy resolution after the absolute calibration are given.

**Table II** Absolute calibration, the energy resolution for different nonuniformities

| Energy | Nonuniformity | | | | |
|--------|------|------|------|------|------|
| [GeV] | 5% | 10% | 15% | 20% | 30% |
| 10 | $3.96 \pm 0.13$ | $4.01 \pm 0.13$ | $4.09 \pm 0.13$ | $4.22 \pm 0.14$ | $4.52 \pm 0.14$ |
| 20 | $2.78 \pm 0.09$ | $2.83 \pm 0.09$ | $2.91 \pm 0.09$ | $3.02 \pm 0.10$ | $3.29 \pm 0.11$ |
| 50 | $1.73 \pm 0.06$ | $1.78 \pm 0.06$ | $1.86 \pm 0.06$ | $1.98 \pm 0.06$ | $2.26 \pm 0.07$ |
| 100 | $1.26 \pm 0.06$ | $1.32 \pm 0.06$ | $1.41 \pm 0.06$ | $1.52 \pm 0.07$ | $1.81 \pm 0.08$ |
| 150 | $1.01 \pm 0.05$ | $1.07 \pm 0.05$ | $1.17 \pm 0.052$ | $1.30 \pm 0.06$ | $1.62 \pm 0.07$ |
| 200 | $0.83 \pm 0.05$ | $0.89 \pm 0.05$ | $1.00 \pm 0.06$ | $1.13 \pm 0.07$ | $1.46 \pm 0.08$ |
| 300 | $0.76 \pm 0.04$ | $0.84 \pm 0.05$ | $0.96 \pm 0.06$ | $1.09 \pm 0.06$ | $1.45 \pm 0.08$ |
| 400 | $0.62 \pm 0.04$ | $0.69 \pm 0.04$ | $0.80 \pm 0.05$ | $0.91 \pm 0.05$ | $1.20 \pm 0.06$ |
| 500 | $0.58 \pm 0.03$ | $0.65 \pm 0.04$ | $0.76 \pm 0.04$ | $0.87 \pm 0.05$ | $1.17 \pm 0.08$ |

From a comparison of Table $II$ data with the corresponding values of the ideal case energy resolution given in Table $I$, one can notice the deterioration in the energy resolution, produced by intrinsic effects of nonuniformity, that increases with $\sigma_{non}$, as expected. In order to express this quantitatively, for each $\sigma_{non}$ the corresponding set of energy resolution values was fitted with a formula as that given by equ.(1), where $b_0$, the intrinsic component, stands here for $b$.

$$\left(\frac{\sigma}{E}\right)_{abs.cal.} = \frac{a}{\sqrt{E}} \oplus b_0 \quad . \tag{13}$$

The results of the fit are given in Table $III$.

**Table III** Absolute calibration, the results of the fit with $a/\sqrt{E} \oplus b_0$

| | Nonuniformity | | | | |
|--------|------|------|------|------|------|
| | 5% | 10% | 15% | 20% | 30% |
| $a$ | $12.35 \pm 0.16$ | $12.55 \pm 0.17$ | $12.81 \pm 0.18$ | $13.24 \pm 0.19$ | $14.06 \pm 0.23$ |
| $b_0$ | $0.14 \pm 0.08$ | $0.32 \pm 0.04$ | $0.51 \pm 0.03$ | $0.67 \pm 0.03$ | $1.06 \pm 0.03$ |
| $\chi^2/ndf$ | 0.72 | 0.60 | 0.58 | 0.71 | 1.23 |

## 3.1 Calibration tower by tower

In this case the calibration coefficients were determined from equ.(6) for $E_0 = 100\ GeV$ and they were used for energy reconstruction at all energies. The calorimeter energy resolution was determined from the calibrated signals following the procedure described previously and the results are given in Table $IV$.

**Table IV** Tower by tower calibration, the energy resolution for different nonuniformities

| Energy | Nonuniformity | | | | |
|--------|------|------|------|------|------|
| [GeV] | 5% | 10% | 15% | 20% | 30% |
| 10 | 3.99 ± 0.09 | 4.12 ± 0.09 | 4.31 ± 0.10 | 4.64 ± 0.10 | 5.30 ± 0.12 |
| 20 | 2.80 ± 0.06 | 2.90 ± 0.07 | 3.05 ± 0.07 | 3.30 ± 0.07 | 3.79 ± 0.09 |
| 50 | 1.71 ± 0.04 | 1.80 ± 0.04 | 1.89 ± 0.04 | 2.04 ± 0.05 | 2.36 ± 0.05 |
| 100 | 1.26 ± 0.06 | 1.32 ± 0.06 | 1.41 ± 0.06 | 1.52 ± 0.07 | 1.81 ± 0.08 |
| 150 | 1.01 ± 0.03 | 1.09 ± 0.03 | 1.20 ± 0.04 | 1.35 ± 0.04 | 1.71 ± 0.05 |
| 200 | 0.84 ± 0.03 | 0.93 ± 0.04 | 1.07 ± 0.04 | 1.25 ± 0.05 | 1.65 ± 0.07 |
| 300 | 0.79 ± 0.03 | 0.93 ± 0.04 | 1.13 ± 0.05 | 1.37 ± 0.06 | 1.88 ± 0.08 |
| 400 | 0.67 ± 0.03 | 0.85 ± 0.04 | 1.08 ± 0.04 | 1.35 ± 0.06 | 1.88 ± 0.08 |
| 500 | 0.61 ± 0.03 | 0.84 ± 0.03 | 1.10 ± 0.05 | 1.40 ± 0.06 | 1.98 ± 0.08 |

A comparison of Table $IV$ results with those from Table $II$ indicates the presence of an additional source of fluctuations which contribute to the energy resolution deterioration. As can be seen, the energy resolution is worse in the case of tower by tower calibration than in absolute calibration and this effect is more pronounced as the energy is further away from the calibration energy $E_0$. According to our treatment, this new energy dependent effect can be taken into account by introducing an additional term (the calibration term $b_c^{tw}$) in the energy resolution parametrisation formula (13) used for the absolute calibration case.

Taking into account the predicted energy dependence of the calibration term given by equ.(12), the Table $IV$ energy resolution values corresponding to a given $\sigma_{non}$ were fitted with:

$$\left(\frac{\sigma}{E}\right)_{tw.cal.} = \frac{a}{\sqrt{E}} \oplus b_0 \oplus c \ln\left(\frac{E}{E_0}\right) \quad . \tag{14}$$

In fig. 5 the energy dependence of energy resolution predicted by equ. (14) for Table $IV$ data is plotted at three values of $\sigma_{non}$: 10%, 20% and 30%. The fig. 5 curves are drawn with fitted parameters given below in Table $V$. On the same picture the curve that fits Table $I$ simulation data for the ideal case (represented by open circles) is also drawn. As a reference value for the real life situation could be
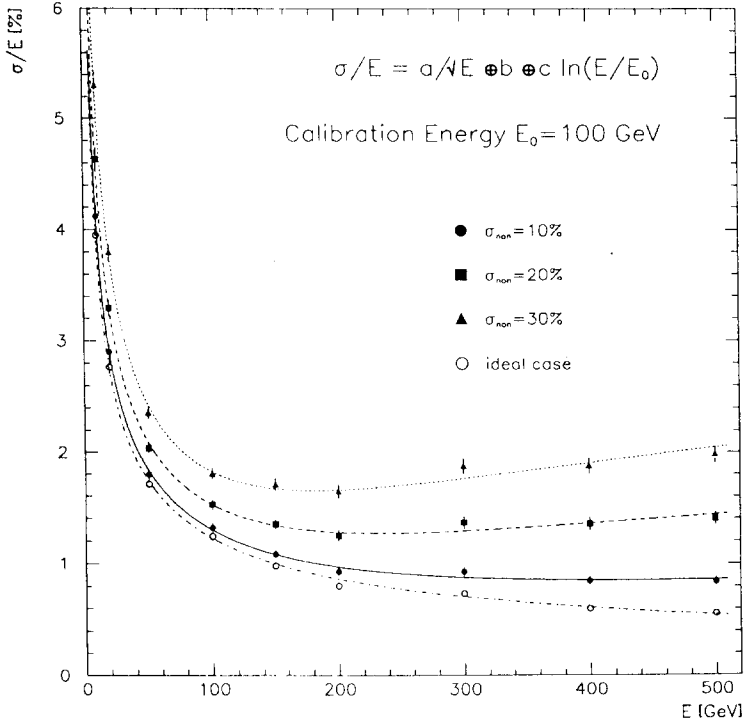
11

**Fig. 5.** Calorimeter energy resolution after tower by tower calibration, for difl ent nonuniformities $\sigma_{non}$.

taken $\sigma_{non} = 10\%$. Recent determinations [7], made by a Florida State Unive group, have given $\sigma_{non} = 7\%$ for the tiles light yield standard deviation.

The fitted parameters for all nonuniformity values are presented in Table V

**Table V** Tower by tower calibration, the results of the fit with
$$a/\sqrt{E} \oplus b_0 \oplus c \ln(E/E_0)$$

| | Nonuniformity | | | | |
|---|---|---|---|---|---|
| | 5% | 10% | 15% | 20% | 30% |
| $a$ | $12.34 \pm 0.14$ | $12.63 \pm 0.19$ | $12.89 \pm 0.20$ | $13.45 \pm 0.23$ | $14.44 \pm 0.$ |
| $b_0$ | $0.14 \pm 0.08$ | $0.29 \pm 0.10$ | $0.53 \pm 0.06$ | $0.71 \pm 0.06$ | $1.11 \pm 0.$ |
| $c$ | $0.18 \pm 0.03$ | $0.36 \pm 0.04$ | $0.50 \pm 0.04$ | $0.68 \pm 0.04$ | $0.99 \pm 0.$ |
| $\chi^2/ndf$ | $0.67$ | $0.60$ | $0.59$ | $0.58$ | $0.81$ |

**12**

The results from the tables $III$ and $V$ indicate that within the errors the obtained values of parameters $a$ and $b_0$ from the fit of absolute calibration and tower by tower calibration data coincide. This might be interpreted as an indication in favour of the hypothesis of two independent components which appear in the $b$ term due to tile to tile nonuniformity and which are added quadratically:

$$b = b_0 \oplus b_c \quad . \tag{15}$$

Table $V$ data permit an investigation of fitted parameters dependence on nonuniformity. Equ.(12) indicates that $c$ depends linearly on $\sigma_{non}$. This is illustrated in fig. 6 where Table $V$ $c$ values were well fitted with $c = 0.034\sigma_{non}$, while the theoretical prediction of equ.(11) is $c = 0.036\sigma_{non}$. In fig. 6 the dependence on $\sigma_{non}$ of the other two parameters $a$ and $b_0$ was also fitted using very simple assumptions.
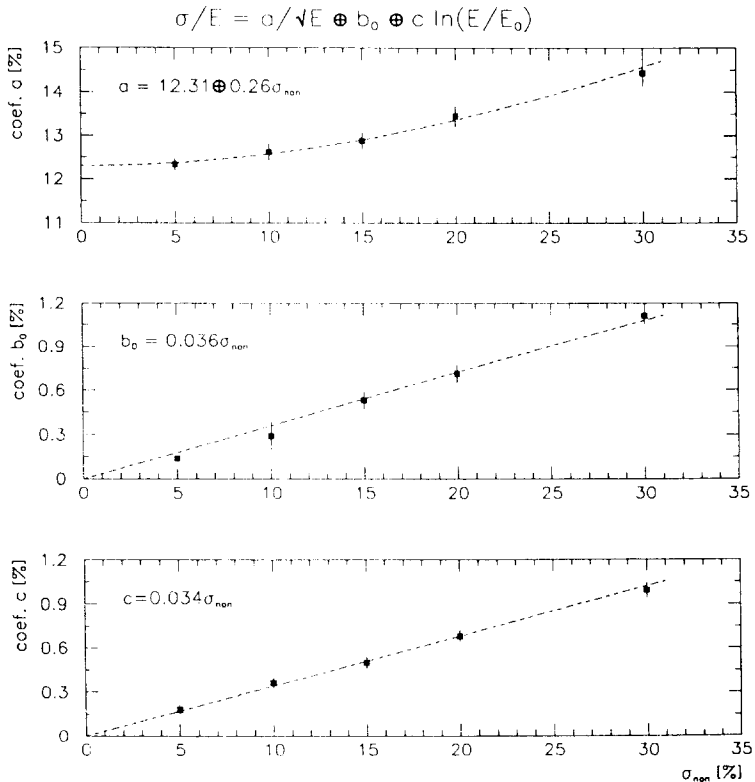


$$\sigma/E = a/\sqrt{E} \oplus b_0 \oplus c \ln(E/E_0)$$

$$a = 12.31 \oplus 0.26\sigma_{non}$$

$$b_0 = 0.036\sigma_{non}$$

$$c = 0.034\sigma_{non}$$

**Fig. 6.** Dependence on $\sigma_{non}$ of the parameters $a$, $b_0$ and $c$ from equ.(14) used to fit the calorimeter resolution in the case of tower by tower calibration;

For example. for $b_0$ we supposed also a linear dependence which was fitted with $b_0 = 0.036\sigma_{non}$. As regards $a$ coefficient. the best fit was obtained supposing that:

$$a = a_0 + a_1 \tag{16}$$

and that $a_1$ depends linearly on $\sigma_{non}$. The fitted $a_0$ value is $a_0 = 12.31 \pm 0.12$, which is consistent within the errors with the value of $a$ that was found in the ideal case. The fitted coefficient of linear dependence of $a_1$ on $\sigma_{non}$ is $0.26 \pm 0.02$.

Some comments are necessary for the unexpected dependence, as it appears at first sight, of the coefficient $a$ on the $\sigma_{non}$. To understand it let us remind how the resolution of the whole calorimeter in the presence of the tile to tile nonuniform response was defined. The calorimeter signal distribution was obtained by collecting the signals from all towers. Because in this case we used the real signals which already incorporate the effect of the tile response nonuniformity, which is normal distributed. this fact manifests itself as if the sampling fraction varies from a tower to another. For the parameter $a$. which characterises the sampling properties of whole calorimeter, this effect appears as an apparent amplification of sampling fluctuations.

Looking at the dependence of the $a$ and $b$ coefficients on $\sigma_{non}$ one can notice that they permit a consistency check of our results: switching off the nonuniformity, the values from the ideal case are reobtained.

The fitted coefficients of the $b_0$ and $c$ linear dependence on $\sigma_{non}$ introduced in the equ.(15) can be used now to evaluate, for the calorimeter considered in this paper. the total contribution of the nonuniformity to the $b$ term for a given energy value. In fig. 7a the $b$ term energy dependence in the $10-500$ GeV range, for different $\sigma_{non}$ values is plotted. A more precise measure of this variation can be expressed by a quantity $\xi(E)$ defined below. which has the property that it is independent of $\sigma_{non}$ :

$$\xi(E) = 100\frac{b(E) - b(E_0)}{b(E_0)} \tag{17}$$

It describes the relative variation of $b$, with respect to its minimum value reached at the calibration energy (i.e. $E_0 = 100 GeV$). In fig. 7b the quantity $\xi(E)$ versus energy $E$ in the $10-500$ GeV range is plotted. A variation of about 80% is observed between 100 and 500 GeV.

Using the knowledge of the energy resolution dependence on $\sigma_{non}$ gained so far. one can extract the value of $b_c^{tw}$ at every energy. A comparison between the obtained and the predicted value might be an additional test of our analytical results.

Taking into account (13) and (14) one can estimate the value of $b_c^{tw}$ from:

$$b_c^{tw} = \sqrt{\left(\frac{\sigma}{E}\right)^2_{tw.cal.} - \left(\frac{\sigma}{E}\right)^2_{abs.cal.}} \tag{18}$$
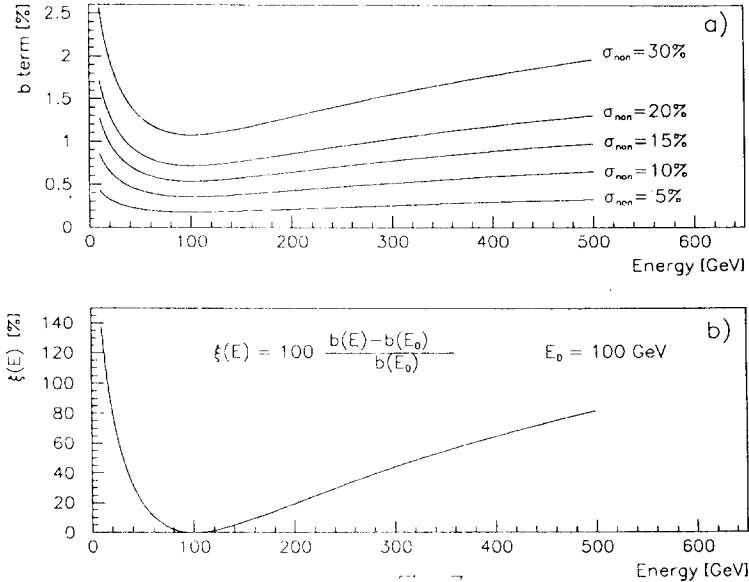
14

**Fig. 7.** (a) total contribution (i.e. $b_0 \div b_c^{tw}$) of tile nonuniformity to the $b$ term for different $\sigma_{non}$ evaluated from results of the fit;

(b) a measure of $b$ variation over the whole energy interval, taking $b(E_0)$ as a reference value.

In the fig. 8 the $b_c^{tw}$ values obtained by this method are plotted. The curves represent the predictions based on equ.(11). One must notice that any free parameter doesn't enter in equ.(11) and the curves are described only in terms of general characteristics of our calorimetertowers: their dimensions, their material physical constants and the tile response nonuniformity. The good description of the simulated data by these curves proves the validity of equ. (11) predictions for calibration term in the case of tower by tower calibration.

## 3.2 Global Calibration

To complete the calibration dependence investigation we also treated the case when a single coefficient $K$ was used to calibrate the response of all towers. The main reason was to obtain an estimation of the level of energy resolution degradation introduced by nonuniformity. After the energy reconstruction, using equ.(5), the energy resolution values were obtained. They are presented in Table $VI$.

15

**Table VI** Global calibration. the energy resolution for different nonuniformities

| Energy [GeV] | Nonuniformity | | | | |
|---|---|---|---|---|---|
| | 5% | 10% | 15% | 20% | 30% |
| 10 | 4.19 ± 0.09 | 4.59 ± 0.10 | 5.45 ± 0.12 | 6.19 ± 0.14 | 8.51 ± 0.19 |
| 20 | 3.01 ± 0.07 | 3.57 ± 0.08 | 4.56 ± 0.10 | 5.35 ± 0.12 | 7.84 ± 0.18 |
| 50 | 2.06 ± 0.05 | 2.76 ± 0.06 | 3.87 ± 0.09 | 4.73 ± 0.11 | 7.34 ± 0.16 |
| 100 | 1.68 ± 0.05 | 2.48 ± 0.07 | 3.62 ± 0.10 | 4.51 ± 0.13 | 7.17 ± 0.21 |
| 150 | 1.48 ± 0.05 | 2.34 ± 0.07 | 3.47 ± 0.11 | 4.41 ± 0.14 | 7.05 ± 0.22 |
| 200 | 1.36 ± 0.05 | 2.26 ± 0.09 | 3.39 ± 0.13 | 4.36 ± 0.17 | 6.98 ± 0.27 |
| 300 | 1.31 ± 0.05 | 2.24 ± 0.09 | 3.36 ± 0.14 | 4.35 ± 0.18 | 6.95 ± 0.28 |
| 400 | 1.23 ± 0.05 | 2.19 ± 0.09 | 3.30 ± 0.13 | 4.31 ± 0.18 | 6.90 ± 0.28 |
| 500 | 1.21 ± 0.05 | 2.18 ± 0.09 | 3.28 ± 0.13 | 4.31 ± 0.18 | 6.89 ± 0.28 |

One can clearly see the resolution deterioration in comparison with ideal case and also with the resolution after tower by tower calibration. This effect is more pronounced for high energies where the systematic effects dominate the energy resolution behaviour and it also increases with nonuniformity. This is due to the $b_c^{gl}$,
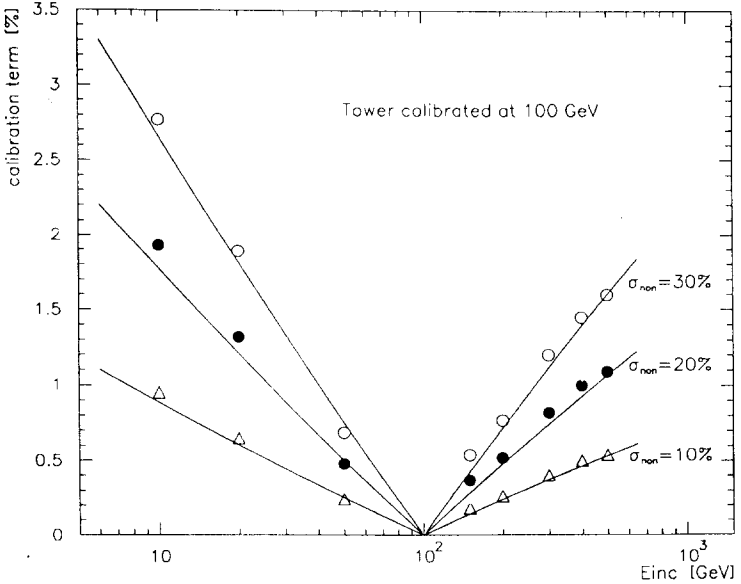


**Fig. 8.** $b_c^{tw}$ vs. incident energy for different $\sigma_{non}$: continuous lines represent analytical formula (11) and the points are obtained using equ.(18) from simulated data.

which - as was predicted [4] (see also fig. 4) - is significantly larger than $b_c^{tw}$. A fit with a formula analogous to (14) where the calibration term is now given by equ.(10) was not able to separate the two contributions of nonuniformity $b_0$ and $b_c^{gl}$ as in tower by tower case due to the very slow energy dependence of $b_c^{gl}$.

What can be done instead, is to use the same procedure as in the case of tower by tower calibration to extract the value of $b_c^{gl}$ at every energy, using a relation similar to equ.(18), which in this case reads:

$$b_c^{gl} = \sqrt{\left(\frac{\sigma}{E}\right)_{gl.cal.}^2 - \left(\frac{\sigma}{E}\right)_{abs.cal.}^2} \quad . \tag{19}$$

In fig. 9 the $b_c^{gl}$ dependence on incident energy for some values of $\sigma_{non}$ is presented. The points were obtained from equ.(19) and the curves represent the equ.(10) predictions. One can notice also the good agreement between the simulated data and the theoretical predictions.
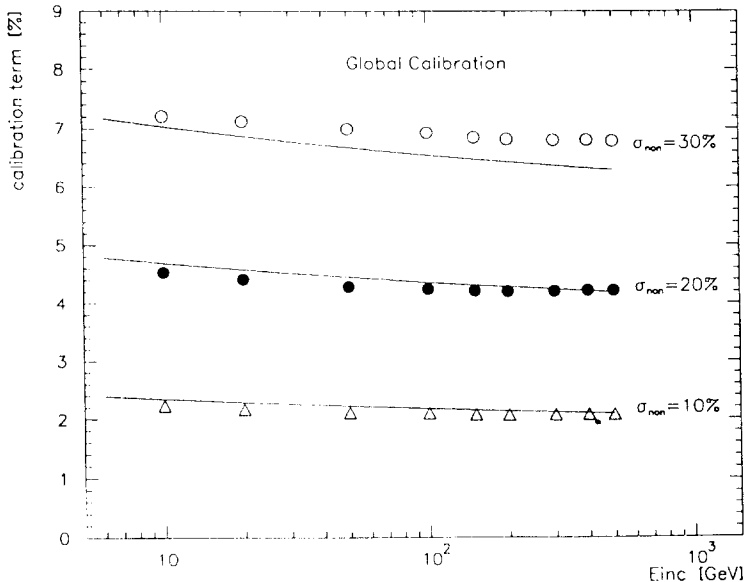


**Fig. 9** $b_c^{gl}$ vs. incident energy for different $\sigma_{non}$: continuous lines represent analytical formula (10) and the points are obtained using equ.(19) from simulated data.

# 4   Conclusions

The influence of the tile to tile nonuniformity on the energy resolution of a sandwich tile electromagnetic calorimeter was investigated in detail. Our treatment was based on the simulation in idealised conditions of a tile calorimeter signal (only sampling has contributed to the energy resolution and all tiles had identical response). Afterwards, on this ideal case results the tile response nonuniformity was superimposed in the form of some weighting factors generated for each tile with a Gaussian distribution with the mean equal to one and with the standard deviation $\sigma_{non}$. The standard deviation $\sigma_{non}$ which measures the degree of the tile response nonuniformity was chosen as a variable to express the variation of calorimeter resolution with nonuniformity. In respect with ideal case a deterioration of calorimeter energy resolution was observed. Both terms of the resolution parametrisation formula were affected, but mostly the systematic term $b$. It was shown that the nonuniformity contributes to $b$ term in two independent ways:

- by broadening the calorimeter signals distribution. This is due to the term $b_0$, that we called intrinsic term, which depends only on $\sigma_{non}$ and this dependence is linear;

- by shifting the mean value of the calorimetric signal distribution. This effect gives another contribution to the systematic term, that we denoted in this paper by $b_c$, which depends also linearly on $\sigma_{non}$, but depends as well on incident energy. The type of $b_c$ energy dependence is different for global and tower by tower calibration.

It was shown that these two terms are added quadratically, i.e. $b = b_0 \oplus b_c$ and the main contribution comes from $b_c$. The $b$ term increases linearly with $\sigma_{non}$ and depends on incident energy. For a fixed $\sigma_{non}$ value, $b$ is significantly smaller in tower by tower calibration than in global calibration.

A method was proposed to separate these two contributions. The obtained $b_c$ values in global and tower by tower calibration were compared with our theoretical predictions [4] and a good agreement was found.

It was also observed a slow increase of the sampling factor $a$ in comparison with the $a_0$ value obtained in the ideal case. The contribution of tile to tile nonuniformity can be represented as an additional term which depends also linearly on $\sigma_{non}$ and is added quadratically to $a_0$.

The present results have a general character and might be valid for a large variety of sampling calorimeters. They have a practical importance for the design of large calorimeters with a good energy resolution.

# References

[1] J. Colas, R. Klanner, J. P. Repellin, T. S. Virdee, Large Hadron Collider Workshop, Aachen, October 1990, CERN 90-10, Volume I, pag.370.

[2] R. Brun et al., GEANT - Cern Program Library, W5013.

[3] J. Proudfoot, Proceedings of the Third International Conference on Calorimetry in High Energy Physics, Corpus Christi, Texas, 1992, edited by Phyllis Halle and James Siegrist, World Scientific, Singapore 1993.

[4] I. Chirikov-Zorin et al., "Influence of Tile Nonuniformity on the Constant Term of E. M. Calorimeter Resolution", Paper submitted to the XXVI International Conference on High Energy Physics, Dallas, 5-12 August 1992, Solenoidal Detector Note, SDC-92-334, a revised version to be published.

[5] Particle Data Group, Phys. Rev. D45 (1992) pag. III.16.

[6] C. Fabjan, in "Experimental Techniques in High Energy Physics", edited by T. Ferbel, Addison-Wesley, 1987.

[7] M. Bertoldi et al., "Machining of Scintillator Tiles for the SDC Calorimeter", Solenoidal Detector Note, SDC-92-289 (1992).

# SUBJECT CATEGORIES
# OF THE JINR PUBLICATIONS

| Index | Subject |
|---|---|
| 1. | High energy experimental physics |
| 2. | High energy theoretical physics |
| 3. | Low energy experimental physics |
| 4. | Low energy theoretical physics |
| 5. | Mathematics |
| 6. | Nuclear spectroscopy and radiochemistry |
| 7. | Heavy ion physics |
| 8. | Cryogenics |
| 9. | Accelerators |
| 10. | Automatization of data processing |
| 11. | Computing mathematics and technique |
| 12. | Chemistry |
| 13. | Experimental techniques and methods |
| 14. | Solid state physics. Liquids |
| 15. | Experimental physics of nuclear reactions at low energies |
| 16. | Health physics. Shieldings |
| 17. | Theory of condensed matter |
| 18. | Applied researches |
| 19. | Biophysics |

Будагов Ю. и др.  E1-94-436
Влияние неоднородностей на энергетическое
разрешение электромагнитных сэмплинг-калориметров

Промоделирован отклик электромагнитного калориметра на электроны с энергиями 10—500 ГэВ. Детально исследовано влияние неоднородного отклика пластин калориметра на коэффициенты $a$ и $b$ в формуле параметризации энергетического разрешения калориметра. Ухудшение энергетического разрешения, связанное с неоднородностями, можно уменьшить с помощью калибровки каждой башни калориметра. Получена явная зависимость коэффициентов $a$ и $b$ от с.к.о. неоднородности отклика пластины. Наши предыдущие результаты по этой зависимости, полученные с помощью аналитических методов при использовании универсальной параметризации профиля электромагнитного ливня, находятся в хорошем согласии с результатами моделирования.

Работа выполнена в Лаборатории ядерных проблем ОИЯИ.

Budagov J. et al.  E1-94-436
Effect of Nonuniformity on the Energy Resolution
of E.M. Sampling Calorimeters

The response of a sampling tile electromagnetic calorimeter was simulated for incident electrons in 10—500 GeV energy range. The influence of tile to tile nonuniformity on the $a$ and $b$ coefficients of the calorimeter energy resolution parametrisation formula was investigated in detail. An energy resolution deterioration due to nonuniformity was observed, but it was shown that the tower by tower calibration can reduce this undesirable effect to reasonable limits. An explicit $a$ and $b$ coefficients dependence on $\sigma_{non}$, the tile response nonuniformity standard deviation, was found. Our previous results on this dependence obtained by analytical methods using the electromagnetic shower mean profile universal parametrisation and the present results obtained by Monte Carlo simulation are compared and found in good agreement.

The investigation has been performed at the Laboratory of Nuclear Problems, JINR.

Редактор Э.В.Ивашкевич. Макет Р.Д.Фоминой